What does this mean? It is possible that for some unknown reason the Majorana zero modes are more stable and occur under a wider range of conditions than theoretically expected, or that we have been lucky in terms of achieving the necessary conditions in the existing devices. It is also possible that the non-quantized zero-bias peaks reflect ordinary Andreev states instead of Majorana zero modes[30]. Then there is the $4\pi$-periodic Josephson effect[10] that now seems to be a necessary but not a unique consequence of the Majorana zero modes[31] adding into the evidence.

Where do we go from here? It is now thought that an observation of a stable quantized $2e^2/h$ zero-bias peak would constitute a smoking gun proof of the Majorana zero mode; it is generally held true that mimicking this type of exact quantization would be difficult. Experimentally, such an observation using present day devices would require an unrealistically low temperature but can perhaps be achieved in future devices. Absent a single smoking gun experiment the final proof of the Majorana existence will most likely involve a body of additional experimental and theoretical work aimed at verifying various aspects of the Majorana zero modes. These include the already mentioned gap closing at the phase transition to and from the topological phase, better theoretical understanding of the 'soft gap' phenomenon observed using tunnelling spectroscopy, as well as several theoretically proposed tests, argued to be

less ambiguous, but so far unrealized. These include probes of non-locality inherent to the pair of spatially separated Majorana zero modes[32–35] and more ambitiously direct tests of their non-Abelian exchange statistics[36]. Finally, it is likely that in the near future similar experiments will be conducted in topological insulator nanowires. If the signatures of zero modes are observed in these as well then this would add to the evidence in favour of Majorana fermions. Owing to the less restrictive conditions that should prevail in these systems it might be possible to access different regimes and observe, for instance, the quantized zero-bias peak conductance more easily. Given our theoretical understanding of the problem and the mounting experimental evidence it is becoming increasingly difficult to foresee a scenario in which the Majorana zero modes would not underlie at least some of the recent reports. Nevertheless, 75 years after Majorana's historic prediction, the race for the unambiguous detection of these elusive particles continues. ❑

*Marcel Franz is at the Department of Physics and Astronomy, University of British Columbia, Vancouver, British Columbia V6T 1Z1, Canada.*
*e-mail: franz@phas.ubc.ca*

### References
1. Majorana, E. *Nuovo Cimento* **14,** 171–184 (1937).
2. Wilczek, F. *Nature Phys.* **5,** 614–618 (2009).
3. Franz, M. *Physics* **3,** 24 (2010).
4. Stern, A. *Nature* **464,** 187–193 (2010).
5. Nayak, C. *et al. Rev. Mod. Phys.* **80,** 1083–1159 (2008).
6. Mourik, V., Zuo, K., Frolov, S. M., Plissard, S. R., Bakkers, E. P. A. M. & Kouwenhoven, L. P. *Science* **336,** 1003–1007 (2012).
7. Deng, M. T. *et al. Nano Lett.* **12,** 6414–6419 (2012).
8. Das, A. *et al. Nature Phys.* **8,** 887–895 (2012).
9. Finck, A. D. K., Van Harlingen, D. J., Mohseni, P. K., Jung, K. & Li, X. Preprint at http://arXiv.org/abs/1212.1101 (2012).
10. Rokhinson, L. P., Liu, X. & Furdyna, J. K. *Nature Phys.* **8,** 795–799 (2012).
11. Moore, G. & Read, N. *Nucl. Phys. B* **360,** 362–396 (1991).
12. Kitaev, A. *Ann. Phys.* **303,** 2–30 (2003).
13. Read, N. & Green, D. *Phys. Rev. B* **61,** 10267–10297 (2000).
14. Fu, L. & Kane, C. L. *Phys. Rev. Lett.* **100,** 096407 (2008).
15. Sau, J. D., Lutchyn, R. M., Tewari, S. & Das Sarma, S. *Phys. Rev. Lett.* **104,** 040502 (2010).
16. Alicea, J. *Phys. Rev. B* **81,** 125318 (2010).
17. Kitaev, A. Y. *Phys. Usp.* **44,** 131–136 (2001).
18. Lutchyn, R. M., Sau, J. D. & Das Sarma, S. *Phys. Rev. Lett.* **105,** 077001 (2010).
19. Oreg, Y., Refael, G. & von Oppen, F. *Phys. Rev. Lett.* **105,** 177002 (2010).
20. Alicea, J. *Rep. Prog. Phys.* **75,** 076501 (2012).
21. Cook, A. M. & Franz, M. *Phys. Rev. B* **84,** 201105(R) (2011).
22. Cook, A. M., Vazifeh, M. M. & Franz, M. *Phys. Rev. B* **86,** 155431 (2012).
23. Moore, J. E. *Nature* **464,** 194–198 (2010).
24. Hasan, M. Z. & Kane, C. L. *Rev. Mod. Phys.* **82,** 3045–3067 (2010).
25. Rosenberg, G., Guo, H-M. & Franz, M. *Phys. Rev. B* **82,** 041104(R) (2010).
26. Peng, H. *et al. Nature Mater.* **9,** 225–229 (2010).
27. Zhang, D. *et al. Phys. Rev. B* **84,** 165120 (2011).
28. Wimmer, M., Akhmerov, A. R., Dahlhaus, J. P. & Beenakker, C. W. J. *New J. Phys.* **13,** 053016 (2011).
29. Stanescu, T. D., Tewari, S., Sau, J. D. & Das Sarma, S. *Phys. Rev. Lett.* **109,** 266402 (2012).
30. Liu, J., Potter, A. C., Law, K. T. & Lee, P. A. *Phys. Rev. Lett.* **109,** 267002 (2012).
31. Sau, J. D., Berg, E. & Halperin, B. I. Preprint at http://arXiv.org/abs/1206.4596 (2012).
32. Fu, L. *Phys. Rev. Lett.* **104,** 056402 (2010).
33. Das Sarma, S., Stanescu, T. D. & Sau, J. D. *Phys. Rev. B* **86,** 220506 (2012).
34. Sau, J. D., Swingle, B. & Tewari, S. Preprint at http://arXiv.org/abs/1210.5514 (2012).
35. Liu, J., Zhang, F-C. & Law, K. T. Preprint at http://arXiv.org/abs/1212.5879 (2012).
36. Alicea, J., Oreg, Y., Refael, G., von Oppen, F. & Fisher, M. P. A. *Nature Phys.* **7,** 412–417 (2011).

# Skyrmions on the track

### Albert Fert, Vincent Cros and João Sampaio

**Magnetic skyrmions are nanoscale spin configurations that hold promise as information carriers in ultradense memory and logic devices owing to the extremely low spin-polarized currents needed to move them.**

Skyrmions are named after the nuclear physicist Tony Skyrme, who developed a nonlinear field theory for interacting pions in the 1960s and showed that topologically stable field configurations occur as particle-like solutions[1]. The word skyrmion is now used to denote similar mathematical objects in many different contexts, from elementary particles to

liquid crystals, Bose–Einstein condensates and quantum Hall magnets. Magnetic skyrmions are chiral spin structures with a whirling configuration (Fig. 1a–d). As their structure cannot be continuously deformed to a ferromagnetic or other magnetic state, skyrmions are topologically protected and relatively stable structures, in comparison with, for example, magnetic

vortices or bubbles. These spin textures were first observed in 2009[2–4], and have since been intensively investigated because they reveal novel types of chiral magnetic orders induced by the spin–orbit coupling (SOC). Moreover, they are appealing because of their potential applications in novel spintronic devices, for example, information storage or logic devices based
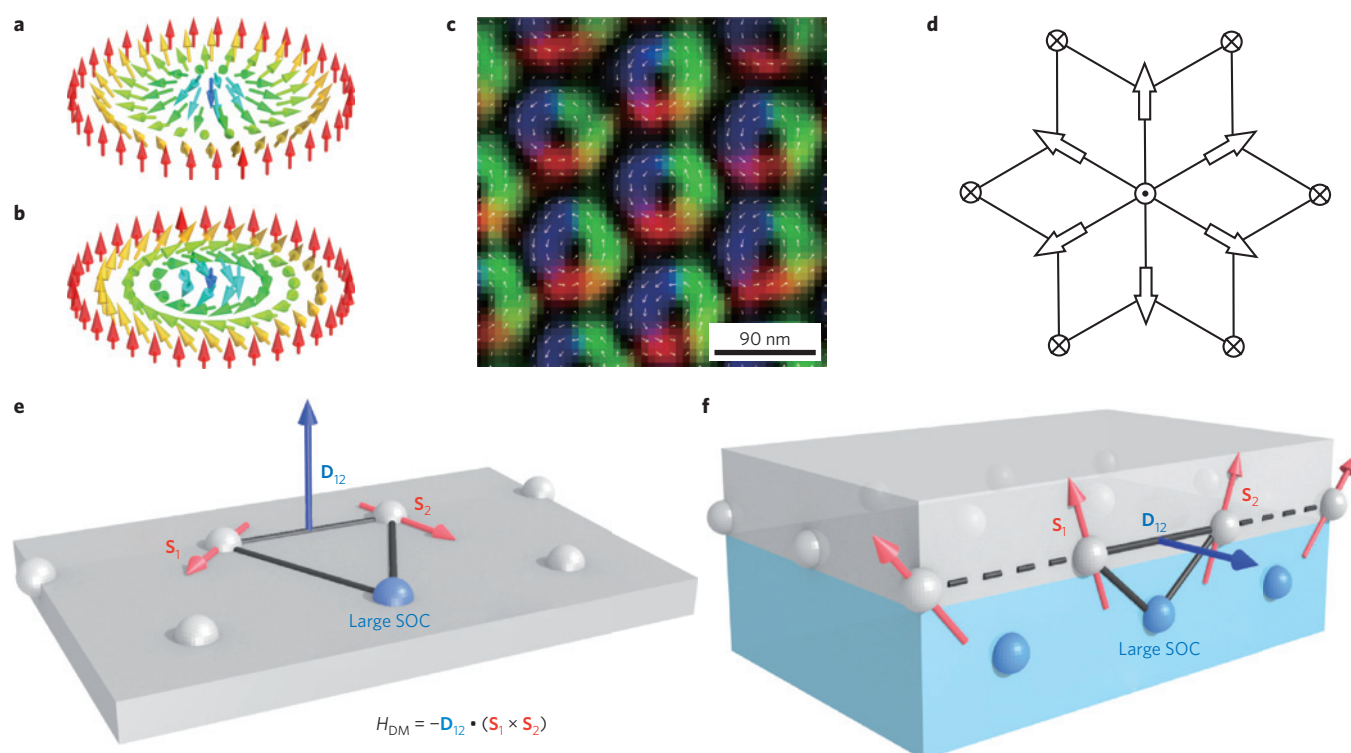
**Figure 1 |** Spins in a skyrmion. **a,b**, Skyrmions in a 2D ferromagnet with uniaxial magnetic anisotropy along the vertical axis. The magnetization is pointing up on the edges and pointing down in the centre. Moving along a diameter, the magnetization rotates by $2\pi$ around an axis perpendicular to the diameter (**a**) and by $2\pi$ around the diameter (**b**), which corresponds to different orientations of the Dzyaloshinskii–Moriya vector. **c**, Lorentz microscopy image[13] of a skyrmion lattice (of the type shown in Fig. 1b) in $Fe_{1-x}Co_xSi$. **d**, Sketch of a nano-skyrmion structure observed in Fe monolayers on Ir(111) (ref. 12). **e**, Schematic of a DMI generated by indirect exchange for the triangle composed of two atomic spins and an atom with a strong SOC[11]. **f**, Sketch of a DMI at the interface between a ferromagnetic metal (grey) and a metal with a strong SOC (blue). The DMI vector $\mathbf{D}_{12}$ related to the triangle composed of two magnetic sites and an atom with a large SOC is perpendicular to the plane of the triangle. Because a large SOC exists only in the bottom metal layer, this DMI is not compensated by a DMI coming from a symmetric triangle[10]. Figure reproduced with permission from: **a,b**, ref. 24, © K. Everschor, Univ. of Köln; **c**, ref. 13, © 2010 NPG; **d**, ref. 12, © 2011 NPG.

on the controlled motion of these particle-like magnetic nanostructures.

Today's hard-disk drives achieve very high densities of information storage, but the complexity and fragility of their mechanical parts motivate the need for solid-state devices with comparable or higher bit densities. The archetype of such devices is the so-called racetrack memory[5] in which the information is coded in a magnetic nanoribbon by a train of up or down magnetic domains separated by domain walls (DWs). The train of DWs can be moved electrically by spin torque to read or write the magnetic information. However, challenges such as reducing the critical currents for DW motion while keeping high velocities and avoiding the detrimental effects of defects must be addressed before this approach can be translated into a competitive technology. The intrinsic properties of magnetic skyrmions might help tackle most of these issues.

## The origin of skyrmions

The spin texture of a magnetic skyrmion[6]

is a stable configuration (or metastable in some cases) that, in most systems investigated up to now, originates from chiral interactions, known as Dzyaloshinskii–Moriya interactions (DMIs)[7–9]. Such interactions are induced because of the lack or breaking of inversion symmetry in lattices or at the interface of magnetic films, respectively. The DMI between two atomic spins $\mathbf{S}_1$ and $\mathbf{S}_2$ can be expressed as: $H_{DM} = -\mathbf{D}_{12} \cdot (\mathbf{S}_1 \times \mathbf{S}_2)$.

For ultrathin magnetic films, which are the main focus here, interfacial DMIs have been predicted[10] from a 3-site indirect exchange mechanism[11] between two atomic spins $\mathbf{S}_1$ and $\mathbf{S}_2$ with a neighbouring atom having a large SOC. The resulting DMI vector is perpendicular to the plane of the triangle (Fig. 1e). At the interface between a ferromagnetic thin layer and a metallic layer with a large SOC, this mechanism generates a DMI for the interface spins $\mathbf{S}_1$ and $\mathbf{S}_2$ with the DMI vector $\mathbf{D}_{12}$ shown in Fig. 1f (ref. 10). The existence of such an interfacial DMI has also been derived from *ab initio* calculations for the Ir(111)/Fe

interface[12]. The magnitude of the interfacial DMI can be very large, ~10–20% of the exchange interaction in analytical calculations[10,11] and up to 30% in *ab initio* calculations[12].

Starting from a ferromagnetic state with $\mathbf{S}_1$ parallel to $\mathbf{S}_2$, the DMI tilts $\mathbf{S}_1$ with respect to $\mathbf{S}_2$ by a rotation around $\mathbf{D}_{12}$. In a two-dimensional (2D) ferromagnet with uniaxial anisotropy and a non-negligible DMI compared with the exchange interaction, the energy is minimized by the skyrmion structure in Fig. 1a for $\mathbf{D}_{12} \perp \mathbf{R}_{12}$ and Fig. 1b for $\mathbf{D}_{12} \parallel \mathbf{R}_{12}$, where $\mathbf{R}_{12}$ is the vector joining the site of $\mathbf{S}_1$ to the site of $\mathbf{S}_2$. The extension of this principle to a 3D lattice is straightforward, the skyrmion structure is obtained by a translation along the anisotropy axis and is made of skyrmion tubes.

A large value of the ratio between $D = |\mathbf{D}_{12}|$ and the exchange coupling $J$ favours a faster rotation of the spin, reducing the skyrmion size (at least in the absence of other interactions like edge effects). The smaller skyrmion size in skyrmion lattices
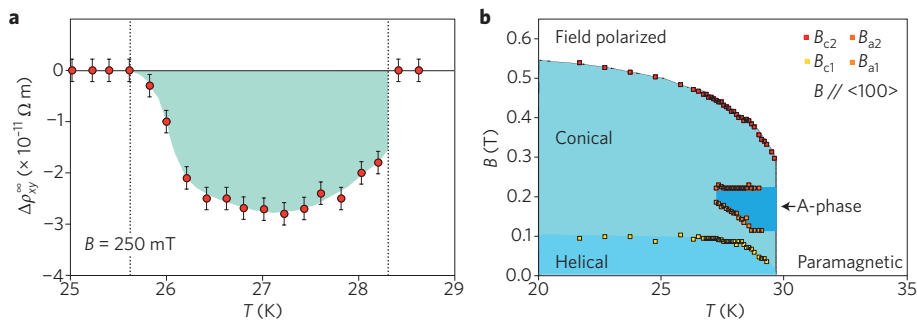
**Figure 2 |** Detection of skyrmions and a phase diagram. **a**, Hall resistivity of MnSi as a function of temperature in the large current limit[19]. The Berry phase collected by electrons going through skyrmions gives rise to a deflection of the charge carriers and to a deviation of the Hall effect (green) from the normal behaviour. **b**, Phase diagram of MnSi (A phase = skyrmion phase)[2]. Figure reproduced with permission from: **a**, ref. 19, © 2012 NPG; **b**, ref. 2, © 2009 AAAS.

of ultrathin films (Fig. 1d) compared with those in bulk materials (Fig. 1c) certainly express larger values of $D/J$ at interfaces. Also, simple energy arguments show that the critical value of $D$ for the existence of skyrmions, $D_{cr}$, depends on both $J$ and the uniaxial anisotropy constant $K$, $D_{cr} \propto (KJ)^{1/2}$, so that, for a $D/J$ characteristic of a given interface, small values of $K/J$ favour the existence of skyrmions.

## Spotted in bulk and thin films
Skyrmion phases have been observed in several bulk materials, including ferromagnets (MnSi (refs 2–4), $Fe_{1−x}Co_xSi$ (refs 13,14), FeGe (refs 15,16)), multiferroics ($Cu_2OSeO_3$; ref. 17), and the antiferromagnet $La_2Cu_{0.97}Li_{0.03}O_4$ (ref. 18). Recently, they have also been observed in ultrathin films[12].

Experimental observations of the formation of a skyrmion lattice in the bulk were first made in MnSi using neutron scattering[2] and confirmed by the detection[3,19] of the so-called topological Hall effect (Fig. 2a). Subsequently, Lorentz microscopy was used to directly image skyrmions in $Fe_{1−x}Co_xSi$ (ref. 13) (Fig.1c). In general, the skyrmion phase in bulk materials is embedded in complex multi-state phase diagrams (Fig. 2b) and it exists only in a relatively narrow range of temperatures and magnetic fields[2,20]. Note that in epitaxial FeGe(111) films ranging from 18 to 300 nm in thickness, the skyrmion phase has recently been stabilized up to 250 K (refs 15,16).

Following observations in the bulk, evidence of skyrmion textures induced by an interfacial DMI in ferromagnetic thin films have been reported by spin-polarized scanning tunnelling microscopy (SP-STM) experiments on Fe monolayers

grown on Ir(111) (ref. 12). The skyrmion lattices are the magnetic ground state of the Fe monolayer so that, in contrast to the general situation in bulk systems, a magnetic field is not required to stabilize the skyrmion phase. These skyrmions are very small (atomic scale, Fig. 1d), in agreement with the very large interfacial DMI predicted by analytical models[10,11] and *ab initio* calculations[12]. There are several other examples of large DMIs at the interface with a heavy metal but these interactions often induce other chiral configurations rather than particle-like skyrmions as, for example, the spin spiral structure found in a Mn monlayer on W(001) (ref. 21). To the best of our knowledge the only published example of interfacial skyrmions is for a Fe monolayer on Ir(111) (ref. 12) but the field has only partially been explored and other interfaces with skyrmions have recently been observed (R. Wiesendanger, personal communication).

## Current-induced motion of skyrmions
Magnetic skyrmions might become the basic building block of a new generation of spintronic devices only if they can be easily inserted in real devices and can be moved or excited at low energy costs. Jonietz et al.[22] observed a current-induced rotation of the orientation of the skyrmion lattice in a B20 MnSi crystal. A temperature or field gradient was necessary to obtain the rotation, and the rotation direction depended on the gradient direction. Very recently, current-induced motion of skyrmions was imaged by Yu et al.[23] using Lorentz microscopy. Concomitantly, Schultz et al.[19] established the correlation between the current-induced motion of the skyrmion lattice in MnSi and

the deviation $\Delta\rho_{xy}$ of the Hall resistivity from the normal behaviour, from which the skyrmion velocity can be estimated (Fig. 3a). Two important comments can be formulated. First, the current densities required to move skyrmions are very small, a few $10^6$ A m$^{-2}$, which is about $10^5$ to $10^6$ smaller than current densities needed to move DWs ($\sim10^{11}$ to $10^{12}$ A m$^{-2}$). Second, the skyrmion velocities in Fig. 3a are small ($\sim10^{-4}$ m s$^{-1}$), and a linear extrapolation indicates that a current density as large as for DWs ($\sim10^{11}$ to $10^{12}$ A m$^{-2}$) would be necessary to reach typical DW velocities of 10–100 m s$^{-1}$. This reflects the fact that the motion is due to the same spin-transfer mechanism in both skyrmions and DWs, and follows the same spin-conservation rules. However, we stress that the important difference is that the depinning current, $j_c$ in Fig. 3a, is greatly reduced in the case of skyrmions, allowing them to move with small currents and small speeds.

For the theory of current-induced motion of skyrmions, we refer to the work of Schultz et al.[19] that is based on Berry phase arguments, and of Everschor et al.[24,25] that uses the Thiele equation to describe the spin dynamics induced by spin torque. Iwasaki et al.[26] compare predictions from the Thiele equation with numerical simulations directly based on the Landau–Lifshitz–Gilbert equation with spin-transfer terms for different non collinear configurations: a skyrmion lattice and a spin helix (that is, series of DWs). Figure 2 in ref. 26 presents the results of simulations with and without pinning, as well as for different values of the damping coefficient $\alpha$ and the non-adiabatic coefficient $\beta$ of the spin-transfer torques. The depinning currents are significant for helical DWs whereas practically zero (at the scale of the figure) for skyrmions. The weak influence of defects is ascribed to the role of the Magnus force for skyrmions and the advantage of their flexibility to avoid pinning centres[26]. Also, the increase of skyrmion velocity with current presents a universal slope whereas it depends on the $\alpha/\beta$ ratio for helical DWs.

As the only results on current-induced motion are for skyrmion lattices, we have performed micromagnetic simulations for individual skyrmions with a modified OOMMF code (J. Sampaio, V. Cros, S. Rohart, A. Thiaville and A. Fert, unpublished observations; see also Fig. 3b,c and Supplementary Movies S1–S3). It turns out that from these new calculations (i) metastable (stable) individual skyrmions can be found in a stable (metastable) ferromagnetic state, (ii) they can be moved by a current along narrow stripes with large

velocities, identical to those of current driven DW motion, (iii) realistic strong pinning sites give rise to depinning currents that are larger than those derived from Hall effect measurements[19] or simulations[26] with skyrmion lattices but are still much smaller than in most experiments with DWs, and (iv) the generation of skyrmions in tracks similar to those in Fig. 3b,c is the next important experimental challenge on the way towards realizing devices. At present, we are using the same types of simulation to test several possible mechanisms (J. Sampaio, V. Cros, S. Rohart, A. Thiaville and A. Fert, unpublished observations).

## Technological interest of skyrmions

The ultimate small size of the skyrmions and the possibility of moving them with electrical currents of very small density make them promising candidates for several types of spintronic storage or logic device[27]. Similar to DW-based racetrack memory, where the information is coded by pairs each consisting of a DW and a magnetic domain, information could be coded by skyrmions in a magnetic nanoribbon. The spacing between bits could be of the order of magnitude of the skyrmion diameter (down to a few nanometres), as in the simulations in Fig. 3b,c. This is much smaller than the spacing between pairs of DWs and magnetic domains in a DW race track (DW widths can also be as small as a few nanometres but the size of magnetic domains can hardly be reduced below 30–40 nm). Although the ratio between velocity $v$ and current density $J$ is not expected to be very different for DWs and skyrmions, smaller sizes and shorter spacings for skyrmions could allow faster information flows with similar current densities, or, alternatively, similar flows with smaller current densities down to the very small depinning currents, leading to lower energy consumption. These advantages might also be exploited in several other spintronic devices such as magnetic random access memories in which a skyrmion is moved into, or out from, one of its electrodes.

The applications described above are implicitly for skyrmions in thin films. Until now, however, skyrmions have only been observed in crystals without inversion symmetry at temperatures below room temperature, and up to 250 K in FeGe (refs 15,16). Room-temperature observations are still also lacking for interface-induced skyrmions as the SP-STM experiments, for technical reasons, have always been performed at low temperatures. However, from the calculated
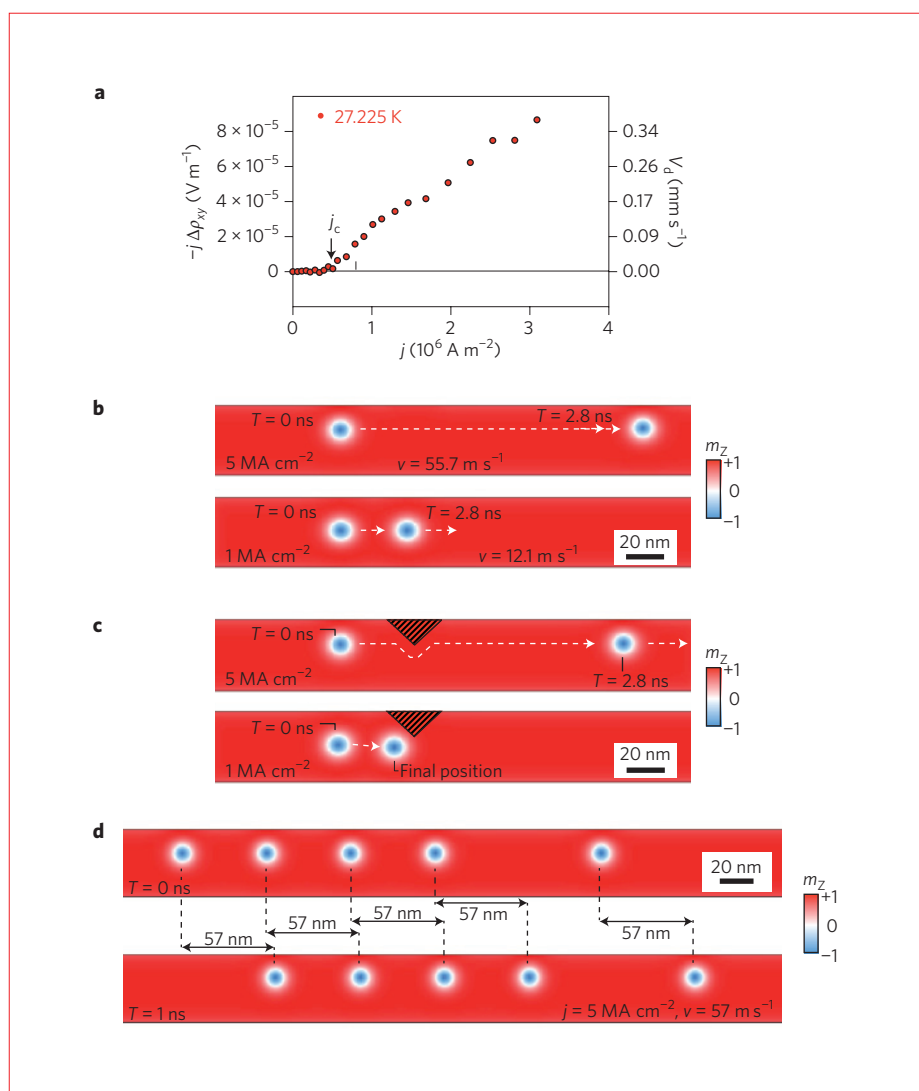


**Figure 3 | Skyrmion velocity. a**, Deviation of the MnSi Hall resistivity from the normal behaviour (left $y$-axis), and the calculated corresponding velocity of the skyrmion lattice along the current direction (right $y$-axis) as a function of the current[19,24]. $j_c$, depinning current. **b–d**, Micromagnetic simulations of current-induced motion of individual skyrmions or chains of skyrmions in $500 \times 40 \times 0.4$ nm³ Co stripes with DMI of 1.4 meV per atom for the interface atoms and the different spin current densities indicated. The positions are indicated at $t = 0$ and either $t = 2.8$ ns or 1 ns, the corresponding velocity is also shown. **b,c**, Individual skyrmions in perfect stripes (**b**) and stripes with pinning (**c**) shown by the shaded triangle of enhanced anisotropy ($j_c$ is between the two current values). **d**, Individual skyrmions and chains of skyrmions exhibit the same velocity. The spacing between skyrmions can be smaller than shown in the figure and of the order of their diameter. The colour scale shows the out-of-plane component of magnetization, $m_z$. Animations of **b–d** can be seen in Supplementary Movies S1–S3. Figure reproduced from: **a**, ref. 19, © 2012 NPG.

stabilization energy[12], skyrmions in Fe on Ir(111) are expected to be stable at room temperature, also demonstrated by the micromagnetic simulations we performed with realistic DMIs. Also considering the unexplored possibilities of multilayered structures with active interfaces, we are reasonably optimistic on the potential of interface-induced skyrmions. In our opinion, the best solution should not be

ultrathin layers like those used in the SP-STM experiments but slightly thicker layers in which the dilution of the interface effect could produce metastable individual skyrmions in a stable ferromagnetic state. Confined geometries like that shown in Fig. 3b–d are of high interest.

## On the road

The exploration of the world of magnetic

skyrmions is just beginning, but it already reveals that these particle-like spin configurations not only raise interesting fundamental problems of chiral magnetic order but also open the way to devices for ultradense information storage and spintronics. On the road to these applications it is now time to proceed from studies on unpatterned samples to the creation and manipulation of individual skyrmions in patterned structures. ❐

*Albert Fert\*, Vincent Cros and João Sampaio are at the Unité Mixte de Physique CNRS/Thales and Université Paris-Sud, Palaiseau, France.*
*\*e-mail: albert.fert@thalesgroup.com*

### References

1. Skyrme, T. H. R. *Nucl. Phys.* **31,** 556–569 (1962).
2. Mühlbauer, S. *et al. Science* **323,** 915–919 (2009).
3. Neubauer, A. *et al. Phys. Rev. Lett.* **102,** 186602 (2009).
4. Pappas, C. *et al. Phys. Rev. Lett.* **102,** 197202 (2009).
5. Parkin, S. S. P., Hayasi, M. & Thomas, L. *Science* **320,** 197202 (2009).
6. Rößler, U. K., Bogdanov, A. N. & Pfleiderer, C. *Nature* **442,** 797–801 (2006).
7. Dzyaloshinskii, I. E. *J. Phys. Chem. Sol.* **4,** 241–255 (1958).
8. Moriya, T. *Phys. Rev.* **120,** 91–98 (1960).
9. Crépieux, A. & Lacroix, C. *J. Magn. Magn. Mater.* **182,** 341–349 (1998).
10. Fert, A. *Mater. Sci. Forum* **59–60,** 439–480 (1990).
11. Fert, A. & Levy, P. M. *Phys. Rev. Lett.* **44,** 1538–1541 (1980).
12. Heinze, S. *et al. Nature Phys.* **7,** 713–718 (2011).
13. Yu, X. Z. *et al. Nature* **465,** 901–904 (2010).
14. Münzer, W. *et al. Phys. Rev. B* **81,** 041203(R) (2010).
15. Yu, X. Z. *et al. Nature Mater.* **10,** 106–109 (2011).
16. Huang, S. X. & Chien, C. L. *Phys. Rev. Lett.* **108,** 267201 (2012).
17. Seki, S. *et al. Science* **336,** 198–201 (2012).
18. Raicevic, I. *et al. Phys. Rev. Lett.* **106,** 227206 (2011).
19. Schulz, T. *et al. Nature Phys.* **8,** 301–304 (2012).
20. Bauer, A. &. Pfleiderer, C. *Phys. Rev. B* **85,** 214418 (2012).
21. Ferriani, P. *et al. Phys. Rev. Lett.* **101,** 027201 (2008).
22. Jonietz, F. *et al. Science* **330,** 1648–1651 (2010).
23. Yu, X. Z. *et al. Nature Commun.* **3,** 988 (2012).
24. Everschor, K. *Current-Induced Dynamics of Chiral Magnetic Structures : Skyrmions, Emergent Electrodynamics and Spin-Transfer Torques.* PhD thesis, University of Köln, Germany (2012).
25. Everschor, K. *et al. Phys. Rev. B* **86,** 054432 (2012).
26. Iwasaki, J., Mochizuki, M. & Nagaosa, N. *Nature Commun.* **4,** 1463 (2013).
27. Kiselev, N. S., Bogdanov, A. N., Schäfer, R. & Rössler, U. K. *J. Phys. D* **44,** 392001 (2011).

### Additional information

Supplementary information is available in the online version of the paper.